COMMISSARIAT A L'ENERGIE ATOMIQUE

CENTRE D'ETUDES NUCLEAIRES DE SACLAY
Service de Documentation
F91191 GIF SUR YVETTE CEDEX

POLARIZATION OBSERVABLES IN ELEMENTARY K^+-PRODUCTION

ADELSECK R.A.- SAGHAI B.
CEA Centre d'Etudes Nucleaires de Saclay, 91 - Gif-sur-Yvette. (FR).
Service de Physique Nucleaire a Haute Energie

POLARIZATION OBSERVABLES IN ELEMENTARY K⁺-PRODUCTION

R.A. Adelseck et B. Saghaï

Service de Physique Nucléaire à Haute Energie, CEN Saclay
91191 Gif sur Yvette cedex, France

POLARIZATION OBSERVABLES IN ELEMENTARY K⁺-PHOTOPRODUCTION[§]

R.A. Adelseck and B. Saghai

DPhN-HE, CEN-Saclay, 91191 Gif-sur-Yvette Cedex, France

The theoretical and experimental status of positive kaon photoproduction off protons from threshold up to 1.4 GeV is briefly reviewed. A model based on Feynman diagrams including several hadronic resonance exchanges is presented. The results of this model are compared with the differential cross section and the Λ-polarization asymmetry data. Predictions on other polarization observables are reported and the need for further measurements is emphasized.

I. INTRODUCTION

The main field of interest in intermediate energy physics has been nucleon-nucleon interactions as well as the properties and the behavior of the first baryonic resonance, where at the subnucleonic level only u- and d-quarks are involved. The quantum number of strangeness brought about by the s-quark introduces a new degree of freedom into this domain. It requires the investigation of hyperon-nucleon (YN) and hyperon-hyperon (YY) interactions, the production and propagation of strange hadronic resonances and strangeness exchange mechanisms.

Reactions like (K^-,π) or (π,K^+) and kaon-nucleon scattering are the most common methods in the domain of strangeness physics, both experimentally and theoretically /Do82/. However, because of the strongly interacting nature of *both* the incident *and* the outgoing particles with the target nucleons the extraction of quantitative informations remains very model dependent.

An attractive alternative to hadronic processes is the use of electromagnetic probes /Co89/. In this procedure, distortions in the incident and outgoing channels are largely reduced due to the rather weakly interacting nature of both the photon and the K⁺ with hadrons. The weakness of these interactions then justifies a first-order theoretical description of the reaction, but results in smaller cross sections than those of hadronic reactions.

After two decades of investigations, the field of the electromagnetic production of strangeness has been dormant since the mid-seventies mainly

due to the lack of adequate experimental facilities. Recent theoretical studies of K⁺ photo- and electroproduction /Co89/ have been motivated by the new generation of accelerators, which will provide continuous, high current and polarized beams in the energy domain of a few GeV; the threshold for the elementary reaction

$$\gamma + p \rightarrow K^+ + \Lambda$$

being at 0.911 GeV.

The effort in understanding kaon photoproduction off the nucleon is crucial in our knowledge of the fundamental KYN coupling constants as well as the reaction mechanisms. Besides, it is a first step in further studies of strangeness in nuclei.

In this contribution we use the most recent model /Ad85, Ad88/ for the photoproduction operator which is based on a few selected first-order Feynman diagrams showing the importance of nucleon-, hyperon-, and kaon-resonance exchange terms. The relevant coupling constants therein are obtained by a phenomenological analysis of the available data.

In the second section we give a short review of the theoretical formalism for the reaction under consideration (a complete description can be found in Ref. /Ad85/). The current status of the experimental situation is summarized in the third section. In the last section we study the sensitivity of different observables to various ingredients of the model. We conclude with suggestions about future experimental studies and possible theoretical improvements.

II. THEORETICAL CONSIDERATIONS

In this section we give a short description of the theoretical technique employed in our study of the elementary process $\gamma + p \rightarrow K^+ + \Lambda$. We recall that the methods used in the theoretical investigation of kaon photoproduction can be classified into three different categories:

    a) dispersion relations (e.g. /Ne66/),

    b) multipole analyses (e.g. /Sc70/), and

    c) isobaric models (e.g. /Re72/).

Dispersion relations provide a very powerful tool in the study of pion photoproduction up to the energy region of the Δ-resonance, but they face severe problems in the case of kaon production. The reason being the rather large rest mass of the kaon and the Λ-N mass difference which require a

high threshold energy (W^{cm}_{tnt} = 1610 MeV) and, hence, allow the exchange of numerous particles and resonances even in the unphysical region below the KΛ threshold.

The method of multipole analyses requires a large number of free parameters (~ 20) to be adjusted. The phenomenological results obtained by several authors show a too small contribution (~ 20%) of the intermediate-state resonances and underestimate the cross section data.

A further shortcoming common to both of these approaches is the non-trivial transformation property of the formalisms. We resolve this problem by applying a diagrammatic technique and, thus, constructing a Lorentz-invariant operator. In this approach, lowest-order Feynman diagrams, shown in Figure 1, represent the Born terms and the contributions

Table 1

Particles of interest and low spin resonances up to 1800 MeV /Ag86/.

Particle	J^π	Mass (MeV)	Width (MeV)
p	1/2⁺	938.2796	
K⁺	0⁻	493.667	
Λ	1/2⁺	1115.6	
Σⁿ	1/2⁺	1192.46	
K⁺⁺	1⁻	892.1	51.3
K1(1280)	1⁺	1260 to 1280	70 to 110 (90)
N1(1440)	1/2⁺	1400 to 1480	120 to 350 (200)
N2(1520)	3/2⁻	1510 to 1530	100 to 140 (125)
N3(1535)	1/2⁻	1520 to 1560	100 to 250 (150)
N4(1650)	1/2⁻	1620 to 1680	100 to 200 (150)
N5(1700)	3/2⁻	1670 to 1730	70 to 120 (100)
N6(1710)	1/2⁺	1680 to 1740	90 to 130 (110)
N7(1720)	3/2⁺	1690 to 1800	125 to 250 (200)
Y1(1405)	1/2⁻	1405	30 to 50 (40)
Y2(1600)	1/2⁺	1560 to 1700	50 to 250 (150)
Y3(1670)	1/2⁻	1660 to 1680	25 to 50 (35)
Y4(1800)	1/2⁻	1720 to 1850	200 to 400 (300)
Y5(1800)	1/2⁺	1750 to 1850	50 to 250 (150)
Y6(1660)	1/2⁺	1630 to 1690	40 to 200 (100)
Y7(1750)	1/2⁻	1730 to 1820	60 to 160 (90)

arising from the excitation of intermediate resonant states, above as well as below the KΛ threshold. The physical values of the states considered in this study are given in Table 1.

Up to now, there exist large discrepancies between KYN coupling constants determined from hadronic interactions with values derived via electromagnetic probes /Ad88/. Even though it is possible to achieve a reasonable fit when the main couplings ($g_{K\Lambda N}$ and $g_{K\Sigma N}$) are constrained to their predicted SU(3) values, the data do not seem to prefer those values when a x^2 analysis is performed (Table 2). The SU(3) symmetry relates the KYN coupling constants /Sw63/ to the well known $g^2_{\pi N N}$ (= 13.90 ± 0.39) /Du83/. Using in addition SU(6) symmetry /Gu64/ yields the following results:

$$\frac{g^2_{K\Lambda N}}{4\pi} = 15.0, \quad \frac{g^2_{K\Sigma N}}{4\pi} = 0.6, \quad \left|\frac{g_{K\Lambda N}}{g_{K\Sigma N}}\right| = 5.0 .$$

The concern of our work is an extensive investigation of the domain of electromagnetic probes. However, for a meaningful comparison more advanced studies in the hadronic field are desirable.

We obtain the coupling constants by performing a phenomenological analysis of the available data /La73/. The currently existing data cover only the domain of differential cross section and final state Λ-polarization asymmetry results. Due to the poor quality of these measurements, especially of the asymmetry data, the parameters cannot be sufficiently constrained. Compared to the differential cross sections, we find polarization observables to be much more selective, but to date only a very restricted number of these experiments has been performed.

Table 2

KΛN and KΣN coupling constants. See text for the explanation of models.

Model	$g_{K\Lambda N}/\sqrt{4\pi}$	$g_{K\Sigma N}/\sqrt{4\pi}$	x^2 *)
1	2.40	-0.0599	8.722
2	1.98	-0.313	6.132
3	4.30	-2.27	4.903

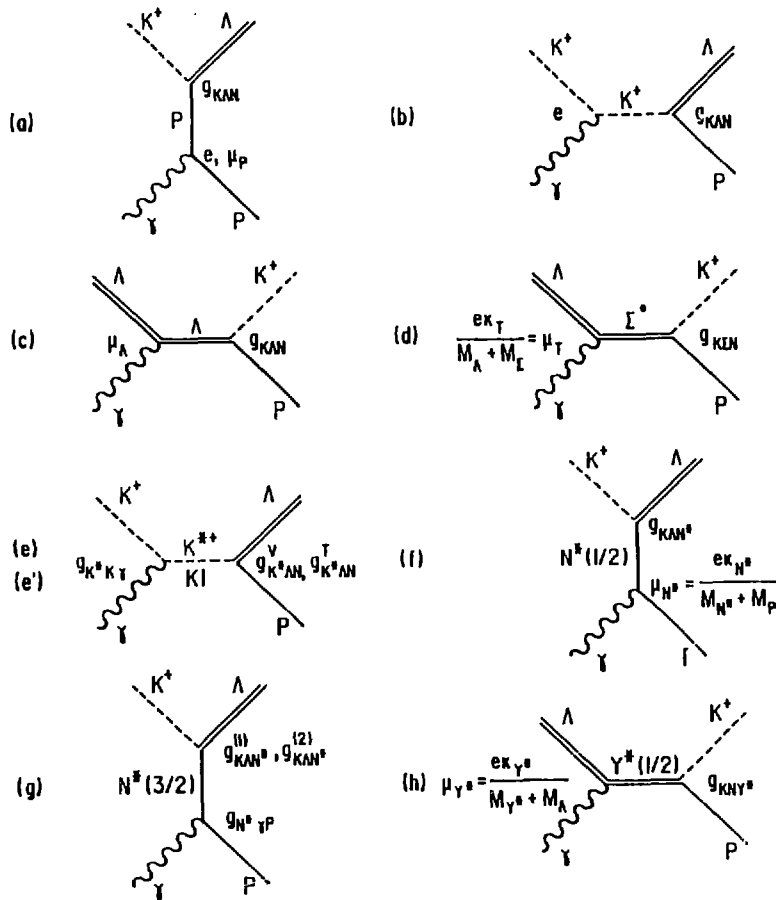*) the fits include all data up to 1.4 GeV; models 1, 2 and 3 contain 4, 6 and 9 free parameters, respectively.

Figure 1 *Feynman diagrams for the process* $\gamma p \rightarrow K^{\cdot} \Lambda$. *(a)-(c) show the Born terms, (d) stands for the* Σ^{0}*-exchange, (e) and (e') represent the spin-1 kaon resonances* $K^{\cdot \cdot}$ *and* $K1$, *(f) and (g) stand for the spin 1/2 and 3/2 nucleon resonances, and (h) represent the spin 1/2 hyperon resonances.*

The numerical values of the $K\Lambda N$ and $K\Sigma N$ coupling constants together with the corresponding reduced χ^2 are shown in Table 2 (where we have used -1.59 μ_N for the Λ-Σ transition moment /Pe86/). The first model contains only the contributions of the diagrams (a)-(d) and the $K^{\cdot \cdot}$ exchange diagram (e) (Figure 1). Model 2 adds diagram (f) coming from the resonances N1 and N4 (Table 1), and Model 3 further includes diagrams (e') and (h) accounting for the exchange of K1 and Y3. Based on χ^2 considerations we do not find much need for the exchange of spin 3/2 nucleonic resonances (diagram (g)) and additional hadronic spin 1/2 resonances, while the inclusion of the K1 resonance improves the fit considerably. In addition, we remark that the $K\Lambda N$ coupling constant approaches its value from hadronic determinations. The still rather large χ^2 is an indication of inconsistencies in the data set.

Due to the poor data we do not attach any significance to the specific values of the remaining terms. However, we do notice that they change smoothly and do not show any erratic behaviour when resonances are being added to the expansion.

The most general cross section for photoproduction of pseudoscalar particles can be written in the form

$$\frac{d\sigma}{d\Omega} = \frac{1}{2} \frac{|\vec{q}|}{k} \operatorname{Tr} \mathcal{F}^{\dagger}\mathcal{F} \quad , \tag{2.1}$$

where

$$\mathcal{F} = \vec{\sigma}.\hat{\epsilon} \; \mathcal{F}_1 \; + \; i(\vec{\sigma}.\hat{q})(\vec{\sigma}.\hat{k}\times\hat{\epsilon}) \; \mathcal{F}_2 \; + \; (\vec{\sigma}.\hat{k})(\hat{\epsilon}.\hat{q}) \; \mathcal{F}_3 \; + \; (\vec{\sigma}.\hat{q})(\hat{\epsilon}.\hat{q}) \; \mathcal{F}_4 \quad . \tag{2.2}$$

The functions $\mathcal{F}_i$ are the CGLN amplitudes /Ch57/, $\hat{k}$ and $\hat{q}$ are unit vectors in the center-of-momentum frame in the direction of the photon and kaon momentum, respectively, and $\hat{\epsilon}$ is the photon polarization vector. The Lorentz-invariant form of the scattering amplitude is given by

$$S_{fi} = \frac{1}{(2\pi)^2} \; \bar{u}(\vec{p}_\Lambda, s_\Lambda) \; \sum_{j=1}^{4} \; A_j M_j \; u(\vec{p}_p, s_p) \; \delta^{(4)}(p_p + p_\gamma - p_K - p_\Lambda) \quad , \tag{2.3}$$

where the matrices M_j and the amplitudes A_j can be found e.g. in Ref. /Ad85/.

As can be seen from Equations (2.2) and (2.3), the most general scattering amplitude is uniquely specified by the knowledge of 4 complex functions. In general, because of the presence of 3 particles with 2 spin

states each, there are $(2^3=)$ 8 amplitudes. Due to parity conservation in electromagnetic interactions, this number is reduced to 4 complex amplitudes /Ja59/. Our goal is to obtain complete information on these functions. Experimentally, this is done by mapping the angular and energy dependence of the amplitudes where for each kinematical choice we need to know 4 complex or equivalently 8 real values. Since we are only able to determine the scattering amplitude up to an overall phase, we thus need 7 independent measurements from which to extract 7 real values.

Because each physical observable is a real bilinear form of the amplitude (2.2), we can construct 16 distinct observables /St67/. These correspond to the differential cross section, single and double polarization processes.

When dealing with polarization observables it is useful to rewrite expression (2.2) in terms of transversity amplitudes where the quantization axis for the proton and lambda spins is parallel to the vector $\hat{k} \times \hat{q}$. Sometimes one may also find the helicity representation useful where the proton and lambda are described by spinors with well defined projections onto their respective momentum vectors. We do not show the analytical expressions at this point but only give a list of all the 16 observables (Table 3) /Ba75/.

The 16 observables shown in Table 3 are not independent. The following nonlinear relations among them can be found:

$$E^2 + F^2 + G^2 + H^2 = 1 + P^2 - \Sigma^2 - T^2 \qquad (2.4)$$

$$FG - EH = P - \Sigma T \qquad (2.5)$$

$$C_x^2 + C_z^2 + O_x^2 + O_z^2 = 1 + T^2 - P^2 - \Sigma^2 \qquad (2.6)$$

$$C_z O_x - C_x O_z = T - P\Sigma \qquad (2.7)$$

$$T_x^2 + T_z^2 + L_x^2 + L_z^2 = 1 + \Sigma^2 - P^2 - T^2 \qquad (2.8)$$

$$T_x L_z - T_z L_x = \Sigma - PT \qquad (2.9)$$

In addition, various inequalities can be derived /Ba75, Go74/ which impose more or less strong bounds on certain observables depending on the numerical values of the others. Thus, given the differential cross section and the three single polarization observables there is still need for three

Table 3

Observables in pseudoscalar meson photoproduction

			Polarization* of		
			γ	p	Λ
1.	$d\sigma/d\Omega$	differential cross section			
	- Single polarization measurements:				
2.	P	lambda polarization asymmetry			y'
3.	Σ	polarized photon asymmetry	p		
4.	T	polarized target asymmetry		y	
	- Double polarization measurements:				
	○ *Beam - Target*				
5.	E		c	z	
6.	F		c	x	
7.	G		t	z	
8.	H		t	x	
	○ *Beam - Recoil*				
9.	C_x		c		x'
10.	C_z		c		z'
11.	O_x		t		x'
12.	O_z		t		z'
	○ *Target - Recoil*				
13.	T_x			x	x'
14.	T_z			x	z'
15.	L_x			z	x'
16.	L_z			z	z'

* quantization axes are defined as follows:

$$\hat{z} : \hat{p}_p , \quad \hat{y} : \hat{p}_\gamma \times \hat{p}_K , \quad \hat{x} = \hat{y} \times \hat{z} ,$$

$$\hat{z}' : \hat{p}_\Lambda , \quad \hat{y}' : \hat{p}_\gamma \times \hat{p}_K , \quad \hat{x}' = \hat{y}' \times \hat{z}' ,$$

p : photon linearly polarized (0, $\pi/2$ w.r.t. scattering plane)

c : photon circularly polarized

t : photon linearly polarized ($\pm \pi/4$ w.r.t. scattering plane)

more measurements of double polarization observables to determine the amplitudes. Due to the relations (2.4-9), these measurements must not all be chosen from the same set (beam-target, beam-recoil or recoil-target). At least one of the experiments must be performed on a different set. The sufficiency of this condition has been shown by Baker et al. /Ba75/. They also demonstrated that these 7 measurements permit the determination of the scattering amplitude only up to quadrant ambiguities. In order to resolve these ambiguities two more experiments are required. Out of the needed five double polarization measurements Baker et al. showed that no four must come from the same set. In summary, to obtain the amplitudes A_j we need to measure 9 out of the possible 16 observables.

Following the framework explained in this section we give estimates on some of the observables' asymmetries in the subsequent sections.

III. EXPERIMENTAL CONSIDERATIONS

The experimental investigation of positive kaon photoproduction started in the late fifties with first and rather poor quality high energy photon beams. At the present time the complete collection of the data /La73/ below 1.4 GeV contains some 140 differential cross section and about 25 final state Λ-polarization asymmetry measurements. Above this energy the data base contains very few points spread over a wide energy range. Hence we restrict our analysis to data within the energy range from threshold up to 1.4 GeV. Presently, there exist no experimental results on the other 14 observables given in Table 3.

It is known that a phenomenological analysis of these data even when combined with the higher energy photo- and/or electro-production measurements does not lead to a satisfactory determination of the free parameters in the theoretical models /Ad88, Sa86/.

Before discussing the need for new measurements we describe briefly a typical experimental method covering the most important features of detection systems as reported in previous studies. Using an electron synchrotron a photon bremsstrahlung beam is obtained with : intensity $\sim 10^9$ equivalent quanta/sec, energy resolution $\sim \pm 25$ MeV and spot size ~ 12 cm^2. The target is a liquid hydrogen target with a thickness of ~ 10 cm.

The crucial point in the identification of kaons is our ability in handling the high background of e^+, μ^+, π^+ and p, mainly due to pion photoproduction reactions, with the ratios N_p/N_K and N_π/N_K being $\sim 10^3$.

Besides, one has to keep in mind the life-times of K' and Λ as well as their main decay channels (say, with braching ratio $\geqslant 1\%$) /Ag86/:

particle	τ (ns)	Mode	Fraction(%)	p (MeV/c)
K'	12.37	$\mu^+\nu$	63.5	236
		$\pi^+\pi^0$	21.2	205
		$\pi^+\pi^+\pi^-$	5.6	125
		$\pi^+\pi^0\pi^0$	1.7	133
		$\pi^0\mu^+\nu$	3.2	215
		$\pi^0 e^+\nu$	4.8	228
Λ	0.26	$p\pi^-$	64.2	100
		$n\pi^0$	35.8	104

For these reasons, the kaons are analysed by a magnetic spectrometer ($\Delta\Omega \sim 3$ msr , $\Delta p/p \sim 5\times10^{-2}$) and identified in a subsequent scintillator counters telescope. In some cases, the experimental set-up is supplemented by differential Cerenkov counter(s) and/or observation of the K-decay particles. The determination of the time of flight (length ~ 5 m, time resolution ~ 500 ps) through the analysing magnet provides a redundance in the selection of kaons and, hence, permits a direct calibration of the K' detection efficiency.

Because of experimental difficulties and low counting rates, the statistical errors range from $\sim \pm 4\%$ to $\pm 10\%$. The systematic uncertainties are reported for only about 2/3 of the data points and are estimated to be $\sim \pm 7\%$ to $\pm 10\%$. So far, in all the phenomenological analyses of the data only statistical errors have been included. This may explain the inconsistencies between different sets of experimental results. A new analysis with more realistic uncertainties taking into account both statistical and systematic errors is in progress and the results will be reported elsewhere.

Compared to the kaon detection, the measurement of the Λ-polarization asymmetry is simpler The protons coming from $\Lambda \rightarrow \pi^- p$ are detected with respect to the kinematic plane by measuring the up-down asymmetry ($\Psi \sim \pm 10°$) in the number of protons using two sets of scintillator (and Cerenkov) counters telescopes without any magnetic analysis. The trigger requires of course a validation from the kaon-arm.

As we mentioned at the beginning of this section, there is a rather large number of differential cross section data. But, on one hand, they
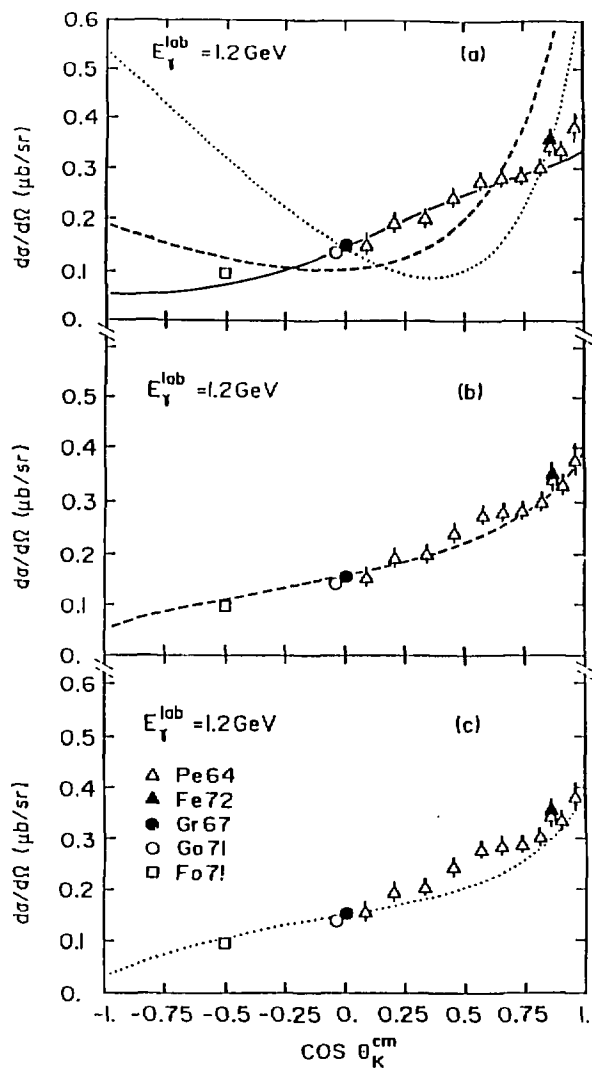
Figure 2 *Comparison of the c.m.s. differential cross section with data. For explanation of curves see the text.*

suffer from the lack of accuracy and, on the other hand, they are scattered into a too large phase space of photon-energy and kaon angle. The only angular distributions with more than 8 points are those at 1.2 and 1.3 GeV. In Fig. 2 we show the results at the lower energy. The solid curve in Fig. 2a as well as the curves in Figures 2b and 2c have been obtained by fitting the complete set of data up to 1.4 GeV and correspond to models 3, 2, and 1, respectively (see Section II and Table 2). Although the comparison between experiment and theory indicates a preference to the most complete model, we are presently not able to conclude on the underlying mechanisms of the reaction. The dashed (dotted) curve in Fig. 2a corresponds to the one shown in Fig. 2b (2c) but using the relevant parameters as determined in model 3. These two curves illustrate the sensitivity of the cross section observable to the model's ingredients.

Figure 3 shows the predictions of models 1 to 3 for the Λ-polarization asymmetry (P) with the appropriate parameters given in Table 2. The data shown in this figure are a collection of all available data for kaon c.m.s. angles between 85° and 95°. Here we see again that the poor quality of the data does not put any severe constraints on the free parameters.
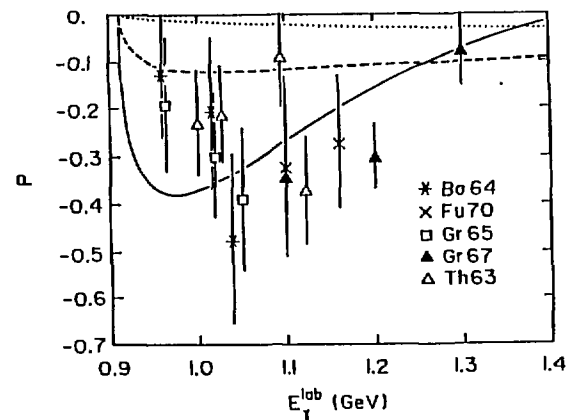

Figure 3 *Comparison of Λ-polarization asymmetry calculated at a kaon cms angle of 90° with data using model 1 (dotted curve), model 2 dashed curve) and model 3 (solid curve).*
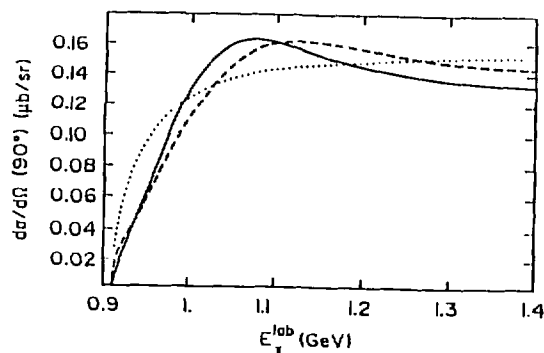
Figure 4 *Energy dependence of the differential cross section at a kaon c.m.s. angle of 90°. The notation agrees with Fig. 3.*

It is obvious that we need more accurate and abundant angular distribution and excitation function data for both $d\sigma/d\Omega$ and P. The present state of the art in experimental nuclear physics (accelerators under construction, thin window liquid targets, detectors, fast electronics and powerful computers) will allow us to reach the desired accuracies (~ ± 5%). The only specific requirement on the experimental set-up is the ability to perform very forward angle measurements both for the kaon and the Λ-decay proton.

IV. PREDICTIONS AND CONCLUSION

In this section we demonstrate the sensitivity of the differential cross section and of a few selected polarization observables to the choice of the particular model (Table 2). This will allow us to study the contributions of the resonant states, thereby obtaining an understanding of their relative importance. It further illustrates the feasibility of measurements and their ability to distinguish between the suggested models.

We explain on two representative figures the dependence on the dominant coupling constant $g_{K\Lambda N}$ by varying this parameter by ± 10%. The purpose of these graphs is to show the sensitivity of the observables to small variations of the K/N coupling.

As we have seen in Figure 2, the available angular distribution data do not discriminate between the differential cross sections predicted by models 1, 2 and 3. To illustrate the energy dependence of the 3 models we show in Figure 4 the differential cross section as a function of photon lab energy up to 1.4 GeV at a fixed kaon c.m.s. angle of 90°.

The most striking feature is the monotonous increase of the differential cross section predicted by model 1, including the Born terms and Σ^* and K^{**} exchange terms. The addition of the nucleon resonances N1 and N4 (model 2) leads to a suppression near threshold as well as at energies above 1.2 GeV. This tendency becomes even more pronounced when we subsequently introduce the resonances Y3 and K1 (model 3). However, the maximum variation of the differential cross section above 1 GeV (at $\theta_K^{c.m.} = 90°$) does not exceed 20%, thus requiring high precision measurements to differentiate between the models.

Analogous to Fig. 2 we present in Figure 5 the predictions for the Λ-polarization asymmetry P (Fig. 5a), the linearly polarized photon asymmetry Σ (Fig. 5b), and the asymmetry of the final-state lambda polarization using a right circularly polarized beam C_x (Fig. 5c). Remarkable are the different predictions of model 3 compared with the simpler models 1 and 2. In particular, the sign change of Σ (Fig. 5b) makes a measurement of this observable highly desirable. In case of the observables P and C_x, the sign of the predicted asymmetries agrees in the three models but the shapes of the curves are sufficiently distinct to allow for identification of the proper model.

In Figure 6 we use model 3 (solid curve) in the calculation of the observables. The dotted (dashed) curve uses the same set of coupling constants as the solid curve except for the value of the K/N coupling constant which has been changed to 3.9 (4.7), i.e. reduced (increased) by 10%. Apart from extreme forward angles, the differential cross section roughly scales with the K/N parameter (Fig. 6a). About the forward direction, the slope of $d\sigma/d\Omega$ appears to be rather sensitive to $g_{K\Lambda N}$. A more substantial reduction of the dominant coupling constant might even result in an inversion of the slope at extreme forward angles. In the remaining region the curves are very similar demanding high precision, absolute measurements of the differential cross section.

The differences in the predictions are more pronounced when looking at the asymmetry parameter C_x (Fig. 6b). A larger coupling constant seems to "smoothen" the asymmetry while a smaller coupling constant increases the variation with angle.
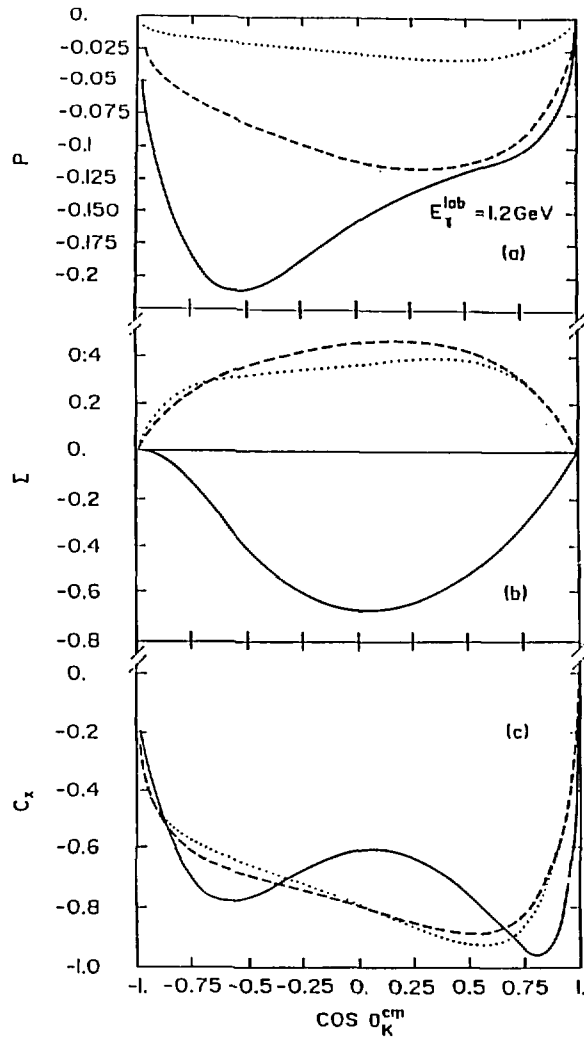
Figure 5 *Angular distribution of the asymmetry observables P, Σ and C_x. The notation agrees with Fig. 3.*
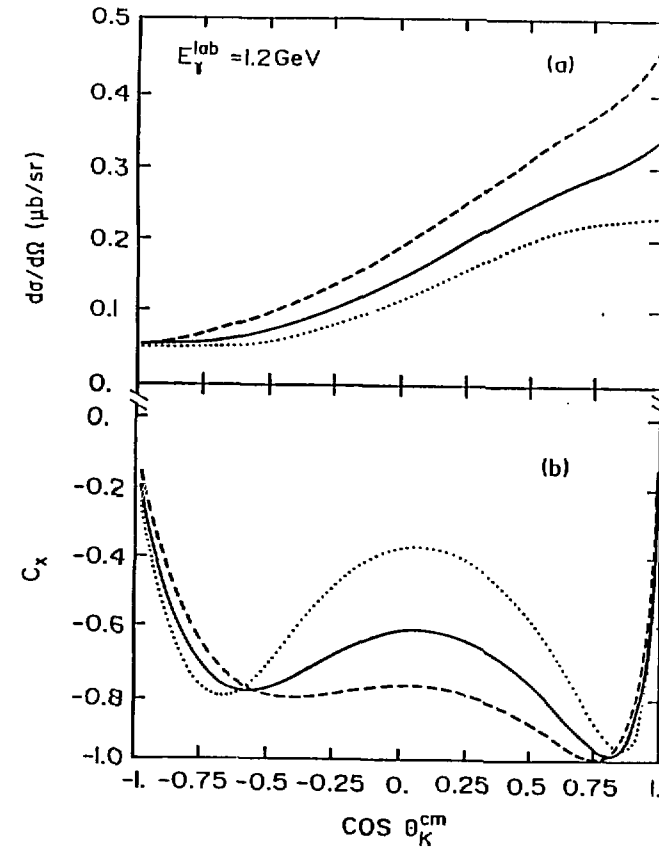
Figure 6 *Angular distribution of the differential cross section and of C_r using model 3 (solid curve). In the calculation of the dotted (dashed) curve the coupling constant g_{KNV} has been reduced (increased) by 10%.*

Special care needs to be taken when interpreting the figures displayed in this section. Because of interference terms, there exists a subtle interplay among the resonances involved in this reaction. Hence, at the present time it is not possible to make a final statement about the absolute values of the asymmetry parameters due to the too large freedom in the choice of the coupling constants. Measurements of polarization observables are indispensable to put strong enough constraints on theoretical models.

The graphs shown in the present contribution are only to be considered as a representative sample of possible measurements. Other observables and other kinematical choices than the ones presented here also offer interesting features. The absence of those graphs in this work does not imply their irrelevance to the questions under consideration.

Concluding, we find that the currently existing data on elementary kaon photoproduction, comprising differential cross section as well as final-state Λ-polarization asymmetry measurements, do not enable us to discriminate between different theoretical models. The reason may be found firstly in the poor quality of the outdated measurements, and secondly in the lack of complete angular distributions and excitation functions. Experiments on the new generation of accelerators employing state-of-the-art detection devices will allow us to significantly improve our understanding of the photoproduction of strangeness. From a theoretical point of view, the effect of $K\Lambda$ final-state interactions /Ta88/ as well as higher order terms needs to be investigated.

REFERENCES

Ad85 R.A. Adelseck et al., Phys. Rev. C32 (1985) 1681.

Ad88 R.A. Adelseck and L.E. Wright, Phys. Rev. C38 (1988) 1965.

Ag86 M. Aguilar-Benitez et al., Particle Data Group, Phys. Lett. 170B (1986)

Ba75 I.S. Barker et al., Nucl. Phys. B95 (1975) 347.

Bo64 B. Borgia et al., Nuovo Cim. 32 (1964) 218.

Ch57 G.F. Chew et al., Phys. Rev. 106 (1957) 1345.

Co89 J. Cohen, Electromagnetic Production of Hypernulei, to be published
in Int. Jour. of Mod. Phys. A (1989)

Do82 C.B. Dover and G.E. Walker, Phys. Rep. 89 (1982) 1.

Du83 O. Dumbrajs et al., Nucl. Phys. B216 (1983) 277.

Fe72 P. Feller et al., Nucl. Phys. B39 (1972) 413.

Fo71 T. Fourneron, Thèse d'Etat, Univ. de Paris, L.A.L. report 1258 (1971)

Fu70 T. Fujii et al., Phys. Rev. D2 (1970) 439.

Go71 H. Going et al., Nucl. Phys. B26 (1971) 121.

Go74 G.R. Goldstein et al., Nucl. Phys. B80 (1974) 164.

Gr65 M. Grilli et al., Nuovo Cim. 38 (1965) 1468.

Gr67 D.E. Groom and J.H. Marshall, Phys. Rev. 159 (1967) 1213.

Gu64 F. Gursey et al., Phys. Rev. Lett. 13 (1964) 173.

Ja59 M. Jacob and G.C. Wick, Ann. Phys. 7 (1959) 404.

La73 Landolt-Börnstein: Numerical Data and Functional Relationships in
Science and Technology (Springer, New York, 1973), Vol. 8.

Ne66 N.F. Nelipa, Nucl. Phys. 82 (1966) 680.

Pe64 C.W. Peck et al., Phys. Rev. 135 (1964) B830.

Pe86 P.C. Petersen et al., Phys. Rev. Lett. 57 (1986) 949.

Re72 Y. Renard, Nucl. Phys. B40 (1972) 499.

Sa86 B. Saghai, in Journées d'études de physique nucléaire sur la photo-
production et l'électroproduction de mésons sur le nucléon
et les noyaux, 29 sept. – 1 oct. 1986 (IPN-Lyon) p. 273.

Sc70 W. Schorsch et al., Nucl. Phys. B25 (1970) 179.

Si67 M. Simonius, Phys. Rev. Lett. 19 (1967) 279.

Sw63 J.J. de Swart, Rev. Mod. Phys. 35 (1963) 916.

Th63 H. Thom et al., Phys. Rev. Lett. 11 (1963) 433.